Published in final edited form as:
Dev Dyn. 2009 February ; 238(2): 351–357. doi:10.1002/dvdy.21835.

Gene Targeted Ablation of High Molecular Weight Fibroblast Growth Factor-2

Mohamad Azhar[1], **Moying Yin**[2], **Ming Zhou**[3], **Hongqi Li**[1], **Marwan Mustafa**[1], **Eyad Nusyr**[1], **Jack B. Keenan**[1], **Hwudaurw Chen**[1], **Sharon Pawlosky**[2], **Connie Gard**[1], **Christina Grisham**[2], **L. Philip Sanford**[1], and **Tom Doetschman**[1,*]

[1]BIO5 Institute, and Department of Cell Biology & Anatomy, University of Arizona, Tucson, AZ

[2]Departments of Molecular Genetics, University of Cincinnati College of Medicine, Cincinnati, OH 45267

[3]Pathology and Laboratory Medicine, Cleveland Clinic, Cleveland, Ohio

Abstract

Fibroblast growth factor-2 (FGF2) is produced as high molecular weight isoforms (HMW) and a low molecular weight isoform (LMW) via alternative usage of translation start sites in a single *Fgf2*mRNA. Although the physiological function of FGF2 and FGF2 LMW has been investigated in myocardial capillarogenesis during normal cardiac growth, the role of FGF2 HMW has not been determined. Here we report the generation of FGF2 HMW-deficient mice in which FGF2 HMW isoforms are ablated by the Tag-and-Exchange gene targeting technique. These mice are normal and fertile with normal fecundity, and have a normal life span. Histological, immunohistochemical and morphometric analyses indicate normal myocardial architecture, blood vessel and cardiac capillary density in young adult FGF2 HMW-deficient mice. These mice along with the FGF2- and FGF2 LMW-deficient mice that we have generated previously will be very useful for elucidating the differential functions of FGF2 isoforms in patho-physiology of cardiovascular diseases.

Keywords

Fibroblast growth factor; high molecular weight isoforms; tag and exchange; knockout mice; cardiac capillary; cardiac hypertrophy; ischemia reperfusion-injury; neurogenesis; bone formation; tumor; angiogenesis; single nucleotide polymorphism

INTRODUCTION

The mouse *Fgf2* gene encodes the HMW and LMW isoforms through alternative protein translation of a single mRNA and are thought to be important for a variety of physiological and pathological processes including those associated with the development and function of cardiovascular system (Liao et al., 2008;Schultz et al., 2002;Yu et al., 2007;Kardami et al., 2007). These FGF2 isoforms are known to exhibit pleiotropic effects (Sorensen et al., 2006). In mouse, the FGF2 LMW isoform (18 kD) is AUG-initiated, whereas FGF2 HMW isoforms (20.5 kD, 21 kD) are produced by utilizing non-canonical CUG codons upstream and in reading frame with the AUG codon, with a nuclear localization signal inbetween (Bugler et al., 1991). Therefore, it is thought that the functional diversity of FGF2 lies not

*Corresponding authors: 1656 E Mabel St, PO Box 245217, Tucson, AZ 85724-5217; Tel - 520-626-4901; Fax – 520-626-7600; Email addresses- tdoetsch@u.arizona.edu (Tom Doetschman); azharm@email.arizona.edu (Mohamad Azhar).

only in the use of multiple signaling pathways (Dailey et al., 2005), but also in differential subcellular distribution into nuclear and cytoplasmic compartments (Sorensen et al., 2006) and a differential ability to be released to the extracellular environment (Florkiewicz et al., 1998). Previous studies suggest that FGF2 HMW is predominantly nuclear, whereas FGF2 LMW colocalizes in the nucleus and cytoplasm and can also be released to the extracellular environment (Davis et al., 1997). We have previously made knockout (KO) mice in which all isoforms of FGF2 are absent (*Fgf2*$^{-/-}$ (Zhou et al., 1998) & *Fgf2*$^{\text{exon 3-ko/exon 3-ko}}$ (Chen et al., 2008)) which demonstrated a role for FGF2 in vascular tone control (Zhou et al., 1998), bone remodeling (Montero et al., 2000;Naganawa et al., 2008;Hurley et al., 2006;Okada et al., 2003) and cortical neurogenesis (Raballo et al., 2000;Vaccarino et al., 1999;Chen et al., 2008). To date, no significant phenotypic differences have been found between these two *Fgf2* KO strains. Mice in which we have ablated just the FGF2 LMW isoform (*Fgf2*$^{\text{lmw-ko/lmw-ko}}$) have indicated a physiological role for the intracellular FGF2 HMW in mediating the effect of estradiol on endothelial cell growth and migration via an intracrine action (Garmy-Susini et al., 2004). Other studies on these mice indicate that FGF2 and FGF2 LMW are important in protection from post-ischemic myocardial dysfunction ([House et al., 2003];Liao et al., 2007). In addition, neither *Fgf2*$^{-/-}$ nor *Fgf2*$^{\text{lmw-ko/lmw-ko}}$ mice nor human *FGF2* transgenic mice had changes in post-ischemic capillary density in the heart (Liao et al., 2007;House et al., 2003), as well as in post-ischemic hind limbs of *Fgf2*$^{-/-}$ mice (Sullivan et al., 2002), though another study did find increased capillary density in other FGF2 overexpression mice (Sheikh et al., 2001). *Fgf2*$^{-/-}$ mice also exhibit reduced cardiac hypertrophy following coarctation (Schultz et al., 1999) or Angiotensin II treatment (Amann et al., 2006). In the latter study, myocardial capillarogenesis was not different between neonatal *Fgf2*$^{+/+}$ and *Fgf2*$^{-/-}$ mice or following hypertrophy, but it was reduced in 4–5-month-old *Fgf2*$^{-/-}$ mice. Finally, if injected into ischemic rat hearts, FGF2 HMW elicits cardiac hypertrophy (Jiang et al., 2007). Taken together, these studies suggest important differential roles for FGF2 isoforms in cardioprotection and cardiac hypertrophy, and in myocardial capillarogenesis in adult mice.

To better understand the physiological function of FGF2 HMW we have used the Tag and Exchange strategy to generate *Fgf2*$^{\text{hmw-ko/hmw-ko}}$ mice in which just the FGF2 HMW isoform is ablated. These mice have no discernable gross or morphological defects and survive normally. Histological examination reveals normal compact and trabeculated myocardium in adult mutant hearts. Morphometric comparison of smooth muscle cell (SMC) myosin and CD34-stained serial sections indicate no significant difference in vessel density and cardiac capillary density between wild type and *Fgf2*$^{\text{hmw-ko/hmw-ko}}$ mice. Collectively, the data indicate that FGF2 HMW is not required for normal cardiac growth and remodeling. Since FGF2 is increasingly considered to have enormous therapeutic potential to treat early and late features of failing hearts (Kardami et al., 2007), these mice should allow us to decipher the pathophysiological function of FGF2 HMW in heart disease, and elucidate the functional diversity of FGF2 in the cardiovascular system.

RESULTS AND DISCUSSION

This is the first report on the generation of mice with a deficiency of the FGF2 HMW. Although we have previously used the Tag and Exchange procedure to produce *Fgf2*$^{-/-}$ and *Fgf2*$^{\text{lmw-ko/lmw-ko}}$ mice (Zhou et al., 1998;Garmy-Susini et al., 2004), we have made significant technical improvement in this procedure in order to generate *Fgf2*$^{\text{hmw-ko/hmw-ko}}$ mice. We have used the *Hprt* gene as both the positive and negative selectable marker for the Tag and Exchange recombination reactions (Fig. 1A), rather than the *neo* and *tk* gene combination originally used (Askew et al., 1993). HPRT-deficient ES cells allow for positive selection with HAT medium and negative selection with 6-TG. The *Hprt* marker gene is a mammalian gene so that it is less amenable to methylation inactivation. One

difficulty that had to be overcome was with the "Exchange" targeting. When the *Hprt* selectable marker gene is inactivated by gene targeting, there will be functional HPRT protein in the cells such that they will be killed by immediate treatment with 6-TG since the half-life of HPRT is 2-3 days (Steen et al., 1991). For this reason we waited 7 days after electroporation before initiating 6-TG selection. The electroporate was immediately plated into 40 60mm plates which were subsequently passaged (1:2) into 40 100mm plates 3 days later and then allowed to growth 4 more days before applying 6-TG. This large number of plates was necessary to prevent colony overgrowth during the selection period and to enable us to determine which resistant colonies were of independent origin. Since spontaneous mutation or loss of the *Hprt* gene occurs at a rate higher than the rate of gene targeting, about 2% of the 6-TG resistant colonies had the desired $Fgf2^{\text{hmw-ko}}$ allele.

$Fgf2^{\text{hmw-ko/hmw-ko}}$ mice (50:50 129 & Black Swiss) were born in a normal (1:2:1) Mendalian ratio. Southern blot analysis, DNA sequencing and *XbaI* digestion of PCR products amplified from genomic DNA confirm the presence of the 14 bp insertion between the CTG and ATG translational start sequences that were designed to block translation of the FGF2 HMW isoforms (Fig. 1C, D and E). Importantly, there are no *LoxP* or *Frt* sites or marker genes in this allele which could inadvertently lead to alterations in regulation or expression of the gene. Successful making of $Fgf2^{\text{hmw-ko/hmw-ko}}$ further exemplifies the usefulness of the Tag and Exchange approach in applying homologous recombination approaches in mouse ES cells to generate new mouse strains containing small genetic polymorphic changes in a given gene. The targeted alleles contain no marker genes and no CRE- or FLP-recombinase recognition sites (*LoxP* or *Frt* sites) which can interrupt important regulatory regions within non-coding gene regions. When one is introducing polymorphisms which may result in subtle phenotypic changes, it is imperative not to leave behind residual sequence changes that in and of themselves could cause subtle phenotypic changes. Thus, the improved Tag and Exchange procedure used here avoids some of the complications of commonly practiced gene targeting approaches.

Western blot analysis on heart tissue demonstrates that no FGF2 isoforms were present in $Fgf2^{-/-}$ mice, that only the LMW isoform was present in $Fgf2^{\text{hmw-ko/hmw-ko}}$ mice, and that only HMW isoforms were present in $Fgf2^{\text{lmw-ko/lmw-ko}}$ mice (Fig. 2A). Western blot analyses of liver and brain tissues further confirmed the complete absence of FGF2 HMW in $Fgf2^{\text{hmw-ko/hmw-ko}}$ mice (Fig. 2B,C). To determine whether $Fgf2^{\text{hmw-ko/hmw-ko}}$ mice were reproductively normal, genotypes of animals that were born from $Fgf2^{\text{hmw-ko/hmw-ko}}$ male to wild-type female crosses (# of crosses = 3, Average litter size = 8 ± 1.53) and from $Fgf2^{\text{hmw-ko/hmw-ko}}$ female to wild-type male crosses (# of crosses = 3, Average litter size = 9 ± 1.00) were determined and compared to the wild-type male to wild-type female crosses (# of crosses = 3, Average litter size = 9.34 ± 0.34). The data showed that all pups from both breeding were heterozygous for $Fgf2^{\text{hmw-ko}}$ allele and that the average litter size is not significantly different from the wild-type crosses ($P = 0.4418$ for KO male × WT female *vs* WT crosses; $P = 0.7676$ for KO female × WT male *vs* WT crosses). This indicates normal fertility and fecundity in homozygous male and female mutant animals. We also observed $Fgf2^{\text{hmw-ko/hmw-ko}}$ mice (n = 4) for about 1.5 year, and longevity was identical to the wild type mice.

Histological examination of myocardium in H & E-stained serial sections of hearts revealed no defects in compact and trabeculated myocardium and myocardial capillarogenesis in $Fgf2^{\text{hmw-ko/hmw-ko}}$ hearts (Fig. 3A–B). The vascular density of SMC-containing blood vessels was quantified in $Fgf2^{\text{hmw-ko/hmw-ko}}$ and wild type mice by SMC myosin staining which stains all coronary vessel walls (Sridurongrit et al., 2008). There was no significant difference in the number of SMC-containing blood vessels per square millimeter (mm^2) between the wild type and $Fgf2^{\text{hmw-ko/hmw-ko}}$ (WT = 6.0788 ± 0.5106/mm^2 *vs* KO = 7.4957

± 0.6783/mm^2, P = 0.1705) hearts (Fig. 3C–F,I). CD34, a reliable marker of cardiac endothelial cells (Pusztaszeri et al., 2006;Amann et al., 2006), was used to determine cardiac capillary density in serial tissue sections. Cardiac capillary density remains unaltered between the wild type and *Fgf2*$^{\text{hmw-ko/hmw-ko}}$ mice (WT = 2853.34 ± 410.74 /mm^2 *vs* KO = 2726.67 ± 157.62/mm^2, P = 0.7877) (Fig. 3G–H,J). Although our data indicate that FGF2 HMW is not required for myocardial capillarogenesis during normal cardiac growth, they do not discount the possibility that altered or pathological amounts of FGF2 HMW may contribute to cardiac pathophysiology, an association seen with cardiac FGF2 injection in cardiac hypertrophy and I–R injury (Jiang et al., 2007). These data are consistent with several published findings which indicate that on 129/Black Swiss (50:50) genetic background the vascular growth was not affected in hearts of *Fgf2*−/− or *Fgf2*$^{\text{lmw-ko/lmw-ko}}$ mice (House et al., 2003;Liao et al., 2007), or in *Fgf2*−/− mouse skeletal muscle (Sullivan et al., 2002). Consistent with the possibility of a role of FGF2 HMW in cardiac pathophysiology, we have recently reported that *Fgf2*$^{\text{hmw-ko/hmw-ko}}$ mice exhibit significant increase in the recovery of postischemic contractile function, whereas 24-kD human FGF2 HMW overexpressing transgenic (*Fgf2*$^{\text{24-kD-hmw TG}}$) mice have significant decrease in postischemic cardiac function after I-R injury (Liao et al., 2008). Collectively, these data along with our recently published findings indicate that FGF2 HMW is not required during physiological cardiac growth and suggest its important role in cardiac pathophysiology.

With the *Fgf2*−/−, *Fgf2*$^{\text{lmw-ko/lmw-ko}}$, *Fgf2*$^{\text{24-kD-hmw TG}}$ and *Fgf2*$^{\text{hmw-ko/hmw-ko}}$ mouse strains we will now be able to make definitive determinations, at the whole animal level and under physiological and disease conditions, concerning many of the outstanding questions about FGF2 isoform function. For example, the data from both *Fgf2*$^{\text{hmw-ko/hmw-ko}}$ and *Fgf2*$^{\text{24-kD-hmw TG}}$ mice suggest a detrimental role of FGF2 HMW isoforms in cardioprotection after I–R injury (Liao et al., 2008), whereas previous findings using both *Fgf2*−/− and *Fgf2*$^{\text{lmw-ko/lmw-ko}}$ mice indicates a beneficial function of FGF2 LMW isoform in cardioprotection after cardiac I-R injury (House et al., 2003). Thus, these mouse models will be useful for investigating the intriguing possibility whether FGF2 HMW and FGF2 LMW isoforms play opposite roles in the pathogenesis of cardiovascular diseases.

There is also little *in vivo* information on questions of intracellular and extracellular isoform localization, trafficking and release. In fact, we have recently demonstrated the utility of these mouse strains by localizing FGF2 isoforms in nonischemic adult mouse hearts (Liao et al., 2008). In wild type hearts, the LMW, 18-kDa isoform was localized to the cytosolic and nuclear fractions of the heart; whereas, the HMW, 20.5 and 21 kDa, isoforms were nuclear localized. In the *Fgf2*$^{\text{lmw-ko/lmw-ko}}$ mice, the HMW isoforms were only expressed in the nucleus. In the *Fgf2*$^{\text{hmw-ko/hmw-ko}}$ mice, the LMW isoform was localized in the cytoplasm and nucleus of the heart. The nuclear localization of the FGF2 LMW isoform may indicate that the FGF2 LMW isoform can elicit its biological activity not only through FGF receptors, but also by acting as a transcription factor or a co-factor in the nucleus to regulate gene expression under normal or stress conditions. These mouse strains will also be useful to determine whether the HMW isoform is released from the cell, and if so, under what conditions (e.g., ischemic stress or hypertrophic stress). With respect to FGF2 isoform function, these mouse strains will enable us to determine which isoforms are involved in cardiac ischemia and hypertrophy, and through which of the FGF2 signaling pathways do these isoforms function in these disorders.

In conclusions, FGF2 has been implicated in embryonic tissue development (Yu et al., 2007;Liao et al., 2008) and a variety of physiological and pathological processes, including cardiac hypertrophy (Schultz et al., 1999;Amann et al., 2006), ischemia/reperfusion injury (Liao et al., 2007;House et al., 2003;Sullivan et al., 2002;Kardami et al., 2007), neuronal regeneration (Vaccarino et al., 1999;Chen et al., 2008;Raballo et al., 2000), bone

development and remodeling (Coffin et al., 1995;Montero et al., 2000;Naganawa et al., 2008;Hurley et al., 2006;Okada et al., 2003), and vascular remodeling and vascular tone control (Zhou et al., 1998). These new mouse strains will provide important insights into the roles of FGF2 isoforms in these biological processes and diseases. They will also provide valuable *in vivo* models for designing careful pre-clinical studies to determine the therapeutic potential of FGF2 isoforms or the targetable pathways through which those isoforms mediate their function in cardiovascular diseases.

EXPERIMENTAL PROCEDURES

Generation of *Fgf2*$^{hmw\text{-}ko/hmw\text{-}ko}$ mice

A modified protocol of the Tag & Exchange strategy that utilized both the positive and negative selection capabilities of the *Hprt* minigene had been used to generate *Fgf2*$^{hmw\text{-}ko/hmw\text{-}ko}$ mice (Askew et al., 1993). The *Fgf2* gene had been previously 'tagged' with an *Hprt* minigene that had replaced exon 1 of the *Fgf2* locus in E14TG2a ES cell lines, thereby producing *Fgf2*−/− mice (Zhou et al., 1998) (Fig. 1A: Tagged allele). We used a mouse genomic library clone (129/J) to produce a targeting vector for the *Fgf2*−/− mice. To generate an 'exchange' targeting vector construct, (Fig. 1A) an oligonucleotide (Oligo) of 14 bp length was inserted into a *SmaI* site located upstream of the canonical ATG start codon (Fig. 1A). This Oligo was designed to introduce stop codons in all 3 reading frames and to cause a frameshift in translation products originating from the non-canonical CTG initiation codons (Fig. 1B). In addition, this Oligo introduced an *XbaI* site as diagnostic for the presence of the insertion (Fig. 1B). No other genetic alterations such as a selection marker or *LoxP* or *Frt* sequences were present in the exchange construct. The exchange construct was linearized with *NotI* and electroporated into 5×10^7 "tagged" (*Fgf2* KO) ES cells.

The ES cells were grown for 9 days in medium containing 1 X HAT (10^{-4} M hypoxanthine, 4×10^{-7} M aminopterin, 1.6×10^{-5} M thymidine, Sigma USA) prior to electroporation with the exchange vector in order to eliminate any cells that had previously picked up spontaneous mutations in the *Hprt* minigene. After electroporation with the exchange vector, the electroporate was plated in 40 60mm tissue culture dishes on HPRT-deficient embryonic fibroblast feeder cells in standard ES cell medium and in the absence of 6-TG. After 3 days the 40 plates were split 1:2 onto 40 100mm plates (with HPRT-deficient feeder cells) and cultured another 4 days in the same medium. At this time (total 7 days after electroporation and without 6-TG) 6-TG was added. 6-TG-resistant colonies were picked on days 7, 8 & 9 of selection. Each colony was plated in one well of a 24-well tray and then processed for genotyping and cryopreserved when confluent. The 7 day waiting period before addition of 6-TG was necessary to allow the residual HPRT protein that was made before inactivation of the minigene to degrade. 6-TG selection resulted in 56 6-TG-resistant clones, one of which (named 9A) was correctly targeted. ES cells were initially screened by PCR using the FGF U11 (forward) and FGF D11 (reverse) primer pair which surround the inserted sequences (Fig. 1A), and PCR products were resolved on 2.5% agarose gels.

The exchanged allele with the 14 bp insertion was confirmed by southern blotting and genomic DNA sequencing using the FGF U11 primer (Fig. 1C–E). Loss of the *Hprt* minigene in the 6-TG resistant 9A clone was also confirmed by PCR using MFGF U1 (forward) & PGK D11 (reverse) primers (Fig. 1A). The forward primer sits upstream of the *Hprt* minigene insertion in the *Fgf2* KO (tagged) allele and the reverse primer sits in the *Hprt* minigene's PGK promoter. This primer pair amplifies a 1.2 Kb band in *Fgf2*−/− mice or E14TG2a cells but produces no band in 9A because the *Hprt* minigene and its PGK promoter is not present in the "exchanged" cell 9A. Cells from 9A were microinjected into C57BL/6 mouse blastocysts. Germline transmission was established by breeding the male ES cell chimeric mice to Black-Swiss females. For genotyping the *Fgf2*$^{hmw\text{-}ko}$ allele, the

FGF U11 and FGF D11 primer pair was used (indicated in Fig. 1A, Exchanged allele), and the PCR products were digested with *XbaI* to confirm the *Fgf2* HMW isoform null allele. This primer pair amplified a 566 bp fragment which was digested into 115 bp and 465 bp fragments due to the presence of a *Xba*I diagnostic site in the targeted 14 bp Oligo (Fig. 1B and E). The PCR amplification procedure used for the *Fgf2* KO locus was described earlier (Zhou et al., 1998). The primer sequences used in this study were as follows: FGF U11 (forward), CCCGCACCCTATCCTTACACA; FGF D11 (reverse), GCCGCTTGGGGTCCTTG; MFGF U1 (Forward), AGGAGGCAAGTGGAAAACGAA; and PGK D1 (Reverse), CCCAGAAAGCGAAGGAACAAA.

DNA sequencing, southern and western blot analyses

Genomic DNA from ES cells or mouse tails was used in a PCR amplification using the U11 and D11 primer pair. The PCR products were purified using PCR purification columns (Qiagen USA), and sequenced using automated sequencers. For Southern blotting, genomic DNA was digested with *XbaI*, *HindIII* and *PstI*, resolved on 0.8% agarose gels, transferred to nylon membranes (GE Healthcare USA), hybridized to ^{32}P-labeled external (Probe A) or internal (Probe B) probes and autoradiographed using Biomax (USA) X-ray films. For western blotting, freshly harvested or frozen hearts, liver and brain from 2 month mice were homogenized in homogenization buffer (20mM Tris, 2mM EDTA, 2M NaCl, 1% NP40, PMSF), and FGF2 was extracted according to published methods (Liao et al., 2007). Rabbit polyclonal antibody to FGF2 (1:1000, Santa Cruz Biotechnology) was used for western blotting. FGF2 blots were visualized by chemiluminescence (Amersham Bioscience).

Histology, immunohistochemistry and morphometric analysis

Transverse tissue sections (5 μm) of paraformaldehyde (4%) fixed and paraffin embedded hearts from 2 month old mice were cut and scored for vascular bed staining (Liao et al., 2007). Histological examination was done on hematoxylin and Eosin (H & E)-stained serial sections. For quantifying blood vessels, serial sections were stained with SMC antibodies (Biomedical Technologies Inc., Cat# BT-564). CD34 antibodies (abcam, USA) were used in immunohistochemical (IHC) staining for marking endothelial capillaries in serial sections of heart. IHC was done by using an LSAB$^+$ kit (Dako, USA). We counted the blood vessels in the entire ventricle in 3 different SMC-stained sections representing 3 different levels in the heart from both wild type and mutants (n = 4). Cardiac capillaries were counted in 5 fields of view per section in 3 different sections representing 3 different levels of the heart (n = 4). All sections were analyzed using bright-field optics with a Zeiss Axio Imager M1 microscope (Carl Zeiss Microimaging, Inc., Thornwood, NY), and morphometric measurements on the captured images was done by AxioVision 4.6.3 imaging software. Microsoft Excel was used for managing the data. Findings are reported as means ± S.E of the mean, and Student's *t*-test (SigmaPlot, Systat Software, Inc., CA) was used for comparing groups. *p*-values were calculated, and a $p<0.05$ was considered significant.

Acknowledgments

We thank all past and present members of Doetschman laboratory, Dr. Jo El Schultz and Janet Bodmer for sharing ideas and technical support. This work was supported by National Institutes of Health Grant 1R01HL070174-03 and the BIO5 Institute (University of Arizona) to T.D., and Arizona Biomedical Research Commission (ABRC #0901) and The Steven M. Gootter Investigator Award for the Prevention of Sudden Cardiac Death to M.A.

REFERENCES

Amann K, Faulhaber J, Campean V, Balajew V, Dono R, Mall G, Ehmke H. Impaired myocardial capillarogenesis and increased adaptive capillary growth in FGF2-deficient mice. Lab Invest. 2006; 86:45–53. [PubMed: 16258522]

Askew GR, Doetschman T, Lingrel JB. Site-directed point mutations in embryonic stem cells: a gene-targeting tag-and-exchange strategy. Molecular & Cellular Biology. 1993; 13:4115–4124. [PubMed: 8391633]

Bugler B, Amalric F, Prats H. Alternative initiation of translation determines cytoplasmic or nuclear localization of basic fibroblast growth factor. Mol Cell Biol. 1991; 11:573–577. [PubMed: 1986249]

Chen K, Ohkubo Y, Shin D, Doetschman T, Sanford LP, Li H, Vaccarino FM. Decrease in excitatory neurons, astrocytes and proliferating progenitors in the cerebral cortex of mice lacking exon 3 from the Fgf2 gene. BMC Neurosci. 2008; 9:94. [PubMed: 18826624]

Coffin JD, Florkiewicz RZ, Neumann J, Mort-Hopkins T, Dorn GW2, Lightfoot P, German R, Howles PN, Kier A, O'Toole BA, Doetschman T. Abnormal bone growth and selective translational regulation in basic fibroblast growth factor (FGF-2) transgenic mice. Molecular Biology of the Cell. 1995; 6:1861–1873. [PubMed: 8590811]

Dailey L, Ambrosetti D, Mansukhani A, Basilico C. Mechanisms underlying differential responses to FGF signaling. Cytokine Growth Factor Rev. 2005; 16:233–247. [PubMed: 15863038]

Davis MG, Zhou M, Ali S, Coffin JD, Doetschman T, Dorn GW. Intracrine and autocrine effects of basic fibroblast growth factor in vascular smooth muscle cells. J Mol Cell Cardiol. 1997; 29:1061–1072. [PubMed: 9160859]

Florkiewicz RZ, Anchin J, Baird A. The inhibition of fibroblast growth factor-2 export by cardenolides implies a novel function for the catalytic subunit of Na+,K+-ATPase. J Biol Chem. 1998; 273:544–551. [PubMed: 9417114]

Garmy-Susini B, Delmas E, Gourdy P, Zhou M, Bossard C, Bugler B, Bayard F, Krust A, Prats AC, Doetschman T, Prats H, Arnal JF. Role of fibroblast growth factor-2 isoforms in the effect of estradiol on endothelial cell migration and proliferation. Circ Res. 2004; 94:1301–1309. [PubMed: 15073041]

House SL, Bolte C, Zhou M, Doetschman T, Klevitsky R, Newman G, Schultz JJ. Cardiac-specific overexpression of fibroblast growth factor-2 protects against myocardial dysfunction and infarction in a murine model of low-flow ischemia. Circulation. 2003; 108:3140–3148. [PubMed: 14656920]

Hurley MM, Okada Y, Xiao L, Tanaka Y, Ito M, Okimoto N, Nakamura T, Rosen CJ, Doetschman T, Coffin JD. Impaired bone anabolic response to parathyroid hormone in Fgf2−/− and Fgf2+/− mice. Biochem Biophys Res Commun. 2006; 341:989–994. [PubMed: 16455048]

Jiang ZS, Jeyaraman M, Wen GB, Fandrich RR, Dixon IM, Cattini PA, Kardami E. High-but not low-molecular weight FGF-2 causes cardiac hypertrophy in vivo; possible involvement of cardiotrophin-1. J Mol Cell Cardiol. 2007; 42:222–233. [PubMed: 17045289]

Kardami E, Detillieux K, Ma X, Jiang Z, Santiago JJ, Jimenez SK, Cattini PA. Fibroblast growth factor-2 and cardioprotection. Heart Fail Rev. 2007; 12:267–277. [PubMed: 17516168]

Liao S, Bodmer J, Pietras D, Azhar M, Doetschman T, Schultz JE. Biological functions of the low and high molecular weight protein isoforms of fibroblast growth factor-2 in cardiovascular development and disease. Dev Dyn. 2008

Liao S, Porter D, Scott A, Newman G, Doetschman T, Schultz JJ. The cardioprotective effect of the low molecular weight isoform of fibroblast growth factor-2: The role of JNK signaling. J Mol Cell Cardiol. 2007; 42:106–120. [PubMed: 17150229]

Montero A, Okada Y, Tomita M, Ito M, Tsurukami H, Nakamura T, Doetschman T, Coffin JD, Hurley MM. Disruption of the fibroblast growth factor-2 gene results in decreased bone mass and bone formation. J Clin Invest. 2000; 105:1085–1093. [PubMed: 10772653]

Naganawa T, Xiao L, Coffin JD, Doetschman T, Sabbieti MG, Agas D, Hurley MM. Reduced expression and function of bone morphogenetic protein-2 in bones of Fgf2 null mice. J Cell Biochem. 2008; 103:1975–1988. [PubMed: 17955502]

Okada Y, Montero A, Zhang X, Sobue T, Lorenzo J, Doetschman T, Coffin JD, Hurley MM. Impaired osteoclast formation in bone marrow cultures of *Fgf2* null mice in response to parathyroid hormone. J Biol Chem. 2003; 278:21258–21266. [PubMed: 12665515]

Pusztaszeri MP, Seelentag W, Bosman FT. Immunohistochemical expression of endothelial markers CD31, CD34, von Willebrand factor, and Fli-1 in normal human tissues. J Histochem Cytochem. 2006; 54:385–395. [PubMed: 16234507]

Raballo R, Rhee J, Lyn-Cook R, Leckman JF, Schwartz ML, Vaccarino FM. Basic fibroblast growth factor (Fgf2) is necessary for cell proliferation and neurogenesis in the developing cerebral cortex. J Neurosci. 2000; 20:5012–5023. [PubMed: 10864959]

Schultz, JJ.; Hoying, JB.; Sullivan, C.; Doetschman, T. FGF and the cardiovascular system. In: Cuevas, P., editor. Fibroblast Growth Factor in the Cardiovascular System. Munich: Holzapfel Publishers; 2002. p. 45-66.

Schultz JJ, Witt SA, Nieman ML, Reiser PJ, Engle SJ, Zhou M, Pawlowski SA, Lorenz JN, Kimball TR, Doetschman T. Fibroblast growth factor-2 mediates pressure-induced hypertrophic response. J Clin Invest. 1999; 104:709–719. [PubMed: 10491406]

Sheikh F, Sontag DP, Fandrich RR, Kardami E, Cattini PA. Overexpression of FGF-2 increases cardiac myocyte viability after injury in isolated mouse hearts. Am J Physiol. 2001; 280:H1039–H1050.

Sorensen V, Nilsen T, Wiedlocha A. Functional diversity of FGF-2 isoforms by intracellular sorting. Bioessays. 2006; 28:504–514. [PubMed: 16615083]

Sridurongrit S, Larsson J, Schwartz R, Ruiz-Lozano P, Kaartinen V. Signaling via the Tgf-beta type I receptor Alk5 in heart development. Dev Biol. 2008

Steen AM, Sahlen S, Lambert B. Expression of the hypoxanthine phosphoribosyl transferase gene in resting and growth-stimulated human lymphocytes. Biochim Biophys Acta. 1991; 1088:77–85. [PubMed: 1703446]

Sullivan CJ, Doetschman T, Hoying JB. Targeted disruption of the Fgf2 gene does not affect vascular growth in the mouse ischemic hindlimb. J Appl Physiol. 2002; 93:2009–2017. [PubMed: 12391121]

Vaccarino FM, Schwartz ML, Raballo R, Nilsen J, Rhee J, Zhou M, Doetschman T, Coffin JD, Wyland JJ, Hung YT. Changes in cerebral cortex size are governed by fibroblast growth factor during embryogenesis. Nat Neurosci. 1999; 2:246–253. [PubMed: 10195217]

Yu PJ, Ferrari G, Galloway AC, Mignatti P, Pintucci G. Basic fibroblast growth factor (FGF-2): the high molecular weight forms come of age. J Cell Biochem. 2007; 100:1100–1108. [PubMed: 17131363]

Zhou M, Sutliff RL, Paul RJ, Lorenz JN, Hoying JB, Haudenschild CC, Yin M, Coffin JD, Kong L, Kranias EG, Luo W, Boivin GP, Duffy JJ, Pawlowski SA, Doetschman T. Fibroblast growth factor 2 control of vascular tone. Nat Med. 1998; 4:201–207. [PubMed: 9461194]

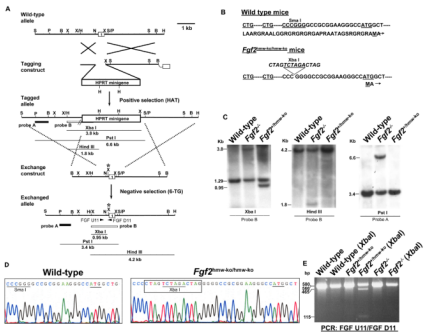

Figure 1. Generation of *Fgf2*$^{\text{hmw-ko/hmw-ko}}$ mice

(A) Tag and Exchange gene targeting strategy and resulting *Fgf2*$^{\text{hmw-ko}}$ exchanged allele. (B) DNA and protein sequence of wildtype and FGF2 HMW KO mice. A 14 bp Oligo containing a *Xba*I site is inserted into Sma I site located 5' upstream of canonical ATG start codon. (C) Southern blot analyses showing mice carrying wild type alleles and knockout alleles (*Fgf2*−/−), and a germline chimeric mouse carrying a successfully targeted exchanged allele (*Fgf2*$^{+/\text{hmw-ko}}$). (D) DNA sequencing of genomic PCR products indicating the presence of 14 bp Oligo with a *Xba*I site and the intact canonical ATG start codon in FGF2 HMW KO mice. (E) PCR Genotyping of germline chimera. Restriction enzyme digestion indicates the presence of a functional *Xba*I site in the *Fgf2*$^{\text{hmw-ko}}$ allele in the germline chimera. Notably, difference in band intensities on this blot is due to unequal loading of protein samples in different lanes. Probes and the expected band size for Southern analysis are indicated in (A). Long arrows in (A) represent MFGF U1 (Forward) and PGK D1 (Reverse) PCR primers used to identify the *Hprt*-tagged allele; arrowheads in (A: Exchanged allele) represent FGF U11 (forward) and FGF D11 (reverse) primers used to identify the targeted exchanged allele. Asterisk in exchange construct and exchanged allele indicates the presence of 14 bp Oligo and *Xba*I site. B, *Bam*HI; H, *Hind*III; N, *Nar*I; P, *Pst*I; S, *Sac*I; Sm, *Sma*I; X, *Xba*I.

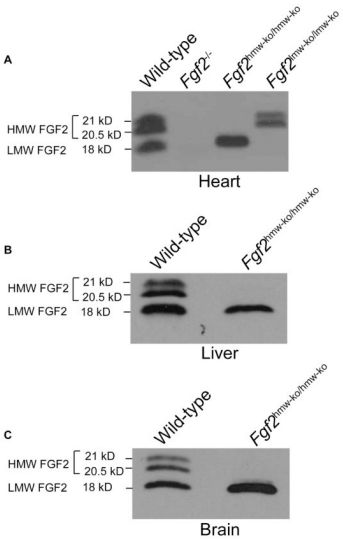

Figure 2. FGF2 HMW protein expression in *Fgf2*$^{\text{hmw-ko/hmw-ko}}$ mice

(A), a representative western blot of heart (A) showing the complete absence of FGF2 HMW isoforms (21 kD & 20.5 kD) in *Fgf2*$^{\text{hmw-ko/hmw-ko}}$, FGF2 LMW isoform (18 kD) in *Fgf2*$^{\text{lmw-ko/lmw-ko}}$ and both HMW (21 kD & 20.5 kD) and LMW (18 kD) isoforms of FGF2 in *Fgf2*−/− hearts mice. Representative western blots also indicate complete absence of FGF2 HMW (21 kD & 20.5 kD) in liver (B) and brain (C) tissues of *Fgf2*$^{\text{hmw-ko/hmw-ko}}$ mice. The blots are representative of at least 3 wild-type/mutant mice pairs.

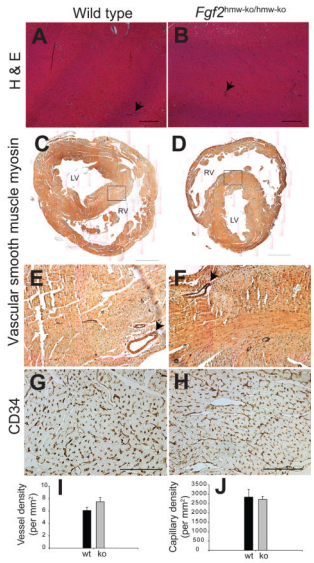

Figure 3. *Fgf2*$^{\text{hmw-ko/hmw-ko}}$ mice (2 month old) have normal myocardial architecture, blood vessel and cardiac capillary density

(**A,B**), H & E stained cross-sections of wild type (A) and *Fgf2*$^{\text{hmw-ko/hmw-ko}}$ (B) mouse hearts. **(C,D)**, SMC myosin immunohistochemistry on wild type (C) and *Fgf2*$^{\text{hmw-ko/hmw-ko}}$ (D) hearts indicating SMC containing blood vessels. Images of the whole heart are reconstructed by combining several smaller images (10×1.6 objective magnification) using Adobe Photoshop. Area under the box in (C) and (D) is magnified and represented by **(E)** and **(F)**, respectively. **(G,H)**, CD34 immunohistochemistry on wild type (G) and *Fgf2*$^{\text{hmw-ko/hmw-ko}}$ (H) hearts depicting cardiac endothelial capillaries. Note that myocardium and myocardial capillarogenesis (arrows, B) is normal in *Fgf2*$^{\text{hmw-ko/hmw-ko}}$ mice. Also, the distribution of SMC containing blood vessels (arrows, D,E) and their quantification (I) is not significantly different between the wild type and *Fgf2*$^{\text{hmw-ko/hmw-ko}}$ mice ($P = 0.1705$). In addition, there is no qualitative (H) and quantitative (J) difference in CD34-stained capillaries between the wild type and *Fgf2*$^{\text{hmw-ko/hmw-ko}}$ mice ($P = 0.7877$). Scale bar: 200 μm (A,B), 1 mm (C,D), 100 μm (G,H). RV, right ventricle; LV, left ventricle.